

A robust PI controller for emulating lateral dynamics of vehicles

C.Villegas, M. Akar, R.N.Shorten, J. Kalkkuhl

Abstract—In this paper we present a framework for vehicle emulation. Based on a decoupling assumption, a robust PI controller is presented for the tracking of predefined vehicle lateral dynamics. Our designs are validated using a full nonlinear vehicle simulator and are shown to be robust to perturbations and capable of providing the basis for emulating a wide range of vehicle types.

I. INTRODUCTION

The availability of 4-wheel-steering (4WS) systems and active suspensions, has made possible the solution of a number of problems in automotive control that have hitherto proved difficult to solve. Among these, vehicle emulation has emerged as a promising solution to an outstanding challenge in the development of ride and handling characteristics for advanced passenger cars: the bridging of the gap between numerical simulations based on a vehicle model — a virtual prototype — and experiments on a proof-of-concept prototype vehicle. An emulating vehicle would act as a generic prototype and would be equipped with advanced computer-controlled actuators enabling it to modify its ride and handling characteristics. Examples of such advanced actuators include 4WS, brake-by-wire and active suspensions. An integrated chassis controller is required to command these actuators to track a set of reference signals corresponding to a desired ride and handling behaviour.

Steps in this direction were started a few years ago by Lee and his coworkers [1], [2]. In [2], Lee demonstrates that a mid-sized test car with 4WS can be used to emulate a small car. The need of a 4WS vehicle is based on its capability to control the lateral motion and the yaw motion independently. A substantial body of research on the control of 4WS cars already exists and a wide variety of control structures have been proposed [3]–[8].

In this paper, we propose a control scheme to track the lateral dynamics of a reference vehicle using 4WS. We demonstrate that a wide range of vehicles can be emulated: from a mini-sized car to a bus, even when the vehicle is subjected to vertical motions, and in the presence of a wide variety of disturbances.

This research was supported by EU Project CEmACS 004175.

C.Villegas is with the Hamilton Institute, NUI Maynooth, Ireland. Carlos.Villegas@nuim.ie

M.Akar was with the Hamilton Institute, NUI Maynooth, Ireland. He is currently with the Department of Electrical and Electronics Engineering, Boğaziçi University, Bebek, İstanbul mehmet.akar@nuim.ie, mehmet_akar@yahoo.com

R.N.Shorten is with the Hamilton Institute, NUI Maynooth, Ireland. Robert.Shorten@nuim.ie

J.Kalkkuhl is with DaimlerChrysler Research, Stuttgart, Germany. jens.c.kalkkuhl@daimlerchrysler.com

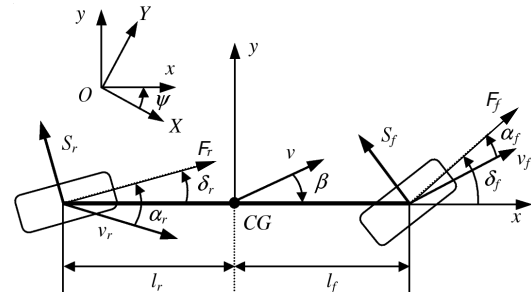


Fig. 1. Single-track model of a 4-wheel steering car

Our paper is structured as follows: in Section II, we describe the one-track vehicle model including lateral force dynamics, caster effect and actuator dynamics. In Section III, the emulation controller is presented and proved to be stable and robust to parameter uncertainty. In Section IV, the stability analysis is extended to time-variations in vehicle speed. In Section V, we present the results for the emulation of different vehicles while performing several driving maneuvers and under the effect of different perturbations in an advanced nonlinear simulation provided by a car manufacturer.

II. LATERAL DYNAMICS MODELLING

We assume that the essential features of the lateral dynamic response of the vehicle to 4WS inputs can be captured using the *single-track model* [4]. In the single-track model, the two wheels at each axle are lumped into a single imaginary wheel located at the centre of the respective axle. The two resulting imaginary wheels are interconnected by a one-dimensional rigid element with the car's mass and moment of inertia around the vertical axis. Furthermore, we assume that the roll, pitch and heave dynamics have a small effect on the lateral dynamics such that they can be neglected. We also assume that the longitudinal speed is constant and that the only forces acting on the single-track model are cornering forces. We refer the interested reader to [9] in order to learn more about the single track model.

Figure 1 depicts the single-track model subject to 4WS inputs. In the figure, l_f (l_r) is the distance from the center of gravity to the front (rear) axle, v is the vehicle speed, ψ is the yaw angle and β is the sideslip angle defined as $\beta = -\frac{v_y}{v_x}$ where v_x and v_y are the components of the vehicle speed v projected to the x and y axis, respectively. Furthermore, δ_f (respectively, δ_r) is the steering angle of both front (rear) wheels and S_f (S_r) is the resultant of the combined cornering forces acting on the front (rear) axle.

The angles α_f and α_r are the front and rear slip angles defined as the angular difference between the orientation of the wheel and the direction of its velocity vector.

We base the design and analysis of the steering controller presented in this paper on a linear time-invariant system describing the single-track model's lateral dynamics at constant longitudinal speed under 4WS. To obtain a state-space representation of such system, we apply the equations of motion of a rigid body to the single-track model. The angles are linearized on the assumption that they will remain small. The system evolves according to the equations:

$$\dot{v}_y = -v_x \dot{\psi} + \frac{S_f + S_r}{m} \quad (1)$$

$$\ddot{\psi} = \frac{S_f l_f - S_r l_r}{I_{zz}} \quad (2)$$

where m is the mass of the vehicle and I_{zz} is its moment of inertia with respect to the vertical axis.

A. Modelling of the cornering forces

When modelling the cornering forces, we consider the dynamics of the force generation at the tyres. Steering inputs do not produce cornering forces instantaneously. The cornering force builds-up approximately as a first order system whose input is the corresponding slip angle.

In addition to the tyre force dynamics, we consider the effect of the caster on the cornering forces generated by the front tyres. Conventional steering systems are designed so that the tyre-road contact point trails behind the steering axis, known as caster trail, and results in a self-aligning torque of the front axle as a reaction to the front-steering input.

Considering the above, we model the total cornering force in the front axle as:

$$\dot{S}_f = a(v_x) \left(2C_T \left(\alpha_f - S_f \frac{n_s}{C_L} \right) - S_f \right) \quad (3)$$

where the parameter $a(v_x)$, which depends on the vehicle speed, is the inverse of the time constant of the first order dynamics describing the tyre force generation; C_T is a constant describing the cornering stiffness of the tyres, n_s is a parameter related to the caster trail and C_L is an elasticity constant of the front steering system. We model the variation of the parameter $a(v_x)$ with the vehicle speed as follows:

$$a(v_x) = \frac{v_x}{a_1 v_x + a_2} \quad (4)$$

where a_1 and a_2 are vehicle dependent parameters (a_1 is given in seconds and a_2 in meters). It can be seen in (3) that we model the effect of the self-aligning torque generated by the caster trail as a dynamic reduction in the effective slip angle at the front wheels.

Since it is assumed that each rear wheel is turned individually by an electro-hydraulic actuator, there is no caster trail at the rear axle. Thus, we model the total cornering force generated at the rear axle as follows:

$$\dot{S}_r = a(v_x) (2C_T \alpha_r - S_r) \quad (5)$$

Considering the geometry of the single-track model and its kinematics as a rigid body, the following expressions for α_f and α_r are obtained assuming small angles:

$$\alpha_f = \delta_f - \frac{v_y + l_f \dot{\psi}}{v_x} \quad (6)$$

$$\alpha_r = \delta_r - \frac{v_y - l_r \dot{\psi}}{v_x} \quad (7)$$

Substituting (6) into (3) and (7) into (5), we obtain the following equations relating the front and rear cornering forces to δ_f and δ_r , respectively:

$$\dot{S}_f = a(v_x) \left(2C_T \left(\delta_f - S_f \frac{n_s}{C_L} - \frac{v_y}{v_x} - \frac{l_f \dot{\psi}}{v_x} \right) - S_f \right) \quad (8)$$

$$\dot{S}_r = a(v_x) \left(2C_T \left(\delta_r - \frac{v_y}{v_x} + \frac{l_r \dot{\psi}}{v_x} \right) - S_r \right) \quad (9)$$

B. Modelling of the steering actuators

We model front and rear steering actuators as second order systems. The input to the front steering actuator is denoted as δ_f^i , and the output is the actual angle by which the two front wheels are turned, δ_f . Both rear steering actuators are modelled as a single second order system whose input is denoted as δ_r^i , and whose output is the steering angle of both rear wheels, δ_r . The transfer functions describing the front and rear actuator dynamics are:

$$\delta_f(s) = \frac{1}{\left(\frac{1}{f_f}\right)^2 s^2 + 2\left(\frac{d_f}{f_f}\right)s + 1} \delta_f^i(s), \quad (10)$$

$$\delta_r(s) = \frac{1}{\left(\frac{1}{f_r}\right)^2 s^2 + 2\left(\frac{d_r}{f_r}\right)s + 1} \delta_r^i(s). \quad (11)$$

C. State-space representation of the system

Considering the above, we can model the lateral dynamics of a vehicle travelling at a given fixed longitudinal speed and subject to 4WS inputs as a linear time-invariant system with two inputs (δ_f^i and δ_r^i) and two outputs (v_y and $\dot{\psi}$). We include below the state-space representation of such system. This representation is obtained by combining equations (1), (2), (8), (9), (10) and (11),

$$\dot{x} = Ax + Bu^i, \quad (12)$$

$$y = Cx + Du^i, \quad (13)$$

where

$$x = [v_y \quad \dot{\psi} \quad S_f \quad S_r \quad \delta_f \quad \dot{\delta}_f \quad \delta_r \quad \dot{\delta}_r]', u^i = \begin{bmatrix} \delta_f^i \\ \delta_r^i \end{bmatrix},$$

$$y = \begin{bmatrix} v_y \\ \dot{\psi} \end{bmatrix}, A = \begin{bmatrix} A_{11} & A_{12} \\ 0_{4 \times 4} & A_{act} \end{bmatrix},$$

$$A_{11} = \begin{bmatrix} 0 & -v_x & \frac{1}{I_{zz}} & \frac{1}{I_{zz}} \\ 0 & 0 & \frac{l_f}{I_{zz}} & -\frac{l_r}{I_{zz}} \\ -\frac{2aC_T}{v_x} & -\frac{2aC_T l_f}{v_x} & -a(1 + 2C_T \frac{n_s}{C_L}) & 0 \\ -\frac{2aC_T}{v_x} & \frac{2aC_T l_r}{v_x} & 0 & -a \end{bmatrix},$$

$$A_{12} = \begin{bmatrix} 0 & 0 & 0 & 0 \\ 0 & 0 & 0 & 0 \\ 2aC_T & 0 & 0 & 0 \\ 0 & 0 & 2aC_T & 0 \end{bmatrix},$$

$$A_{act} = \begin{bmatrix} 0 & 1 & 0 & 0 \\ -f_f^2 & -2d_f f_f & 0 & 0 \\ 0 & 0 & 0 & 1 \\ 0 & 0 & -f_r^2 & -2d_r f_r \end{bmatrix},$$

$$B = \begin{bmatrix} 0 & 0 & 0 & 0 & 0 & f_f^2 & 0 & 0 \\ 0 & 0 & 0 & 0 & 0 & 0 & 0 & f_r^2 \end{bmatrix},$$

$$C = [I_2 \quad 0_{2 \times 6}], \quad D = 0_{2 \times 2}.$$

As indicated above, the vehicle speed v_x is considered as a fixed parameter in the linear model.

III. CONTROL DESIGN

Vehicle reference models are used to convert driver steering wheel angles into reference time-series trajectories for each of the vehicle states. This is depicted in Figure 2. The job of the vertical and lateral controllers is to track these vehicle states. Our basic strategy is to use the 4WS system to track vehicle yaw-rate and sideslip, and the suspension system to track the roll dynamics. In this section, we present a lateral controller design.

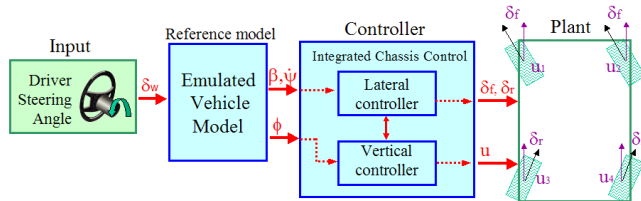


Fig. 2. Emulation Controller Architecture

First, let us assume that the cornering stiffness and actuator dynamics are fast enough to be neglected. Then, for the control design, we get a single-track model of the form:

$$\dot{x} = A_1 x + B_1 \delta^i, \quad (14)$$

where $x = [v_y, \psi]'$, $\delta^i = [\delta_f^i, \delta_r^i]'$ and

$$A_1 = \begin{bmatrix} -\frac{C_f + C_r}{mv_x} & -v_x + \frac{C_r l_r - C_f l_f}{mv_x} \\ \frac{C_r l_r - C_f l_f}{I_{zz} v_x} & -\frac{C_f l_f^2 + C_r l_r^2}{I_{zz} v_x} \end{bmatrix}, \quad (15)$$

$$B_1 = \begin{bmatrix} \frac{C_f}{I_{zz}} & \frac{C_r}{I_{zz}} \\ \frac{C_f l_f}{I_{zz}} & -\frac{C_r l_r}{I_{zz}} \end{bmatrix}, \quad (16)$$

where C_f and C_r are the static cornering stiffness defined by:

$$C_f = \frac{2C_T C_L}{2n_s C_T + C_L}, \quad (17)$$

$$C_r = 2C_T. \quad (18)$$

Now, let us add a feedforward to the vehicle to change our states to be the error between the measured and desired yaw-rate and side-slip states ($e = x - x_{ref}$):

$$\delta^i = B_1^{-1}(\dot{x}_{ref} - A_1 x_{ref}) + \delta_2^i. \quad (19)$$

The resulting error dynamics e :

$$\dot{e} = A_1 e + B_1 \delta_2^i, \quad (20)$$

are modified using our new control inputs δ_2^i to get a system with monotonically decreasing error norm $E = ee'$. This can be done by making the A_1 matrix symmetric with state feedback. We choose to make the A_1 matrix stable and symmetric by changing its upper-right element using yaw-rate. The input required is:

$$\delta_2^i = B^{-1} \begin{bmatrix} \left(\frac{(C_r l_r - C_f l_r)(m - I_{zz})}{m I_{zz} v_x} + v_x \right) \dot{\psi} \\ 0 \end{bmatrix} + \delta_3^i, \quad (21)$$

such that our close-loop plant is: $\dot{e} = A_s e + B_1 \delta_3^i$ where

$$A_s = \begin{bmatrix} -\frac{C_f + C_r}{mv_x} & \frac{C_f l_f - C_r l_r}{I_{zz} v_x} \\ \frac{C_f l_f - C_r l_r}{I_{zz} v_x} & -\frac{C_f l_f^2 + C_r l_r^2}{I_{zz} v_x} \end{bmatrix}. \quad (22)$$

In order to improve the tracking performance and eliminate the steady-state error, we add a PI controller. Consider the control input

$$\delta_3^i = B_1^{-1} \left(K_p e + K_i \int e d\tau \right). \quad (23)$$

The closed-loop system can be thus rewritten as:

$$\begin{bmatrix} \dot{e} \\ \nu \end{bmatrix} = \begin{bmatrix} A_s + K_p & K_i \\ I_2 & 0_{2 \times 2} \end{bmatrix} \begin{bmatrix} e \\ \nu \end{bmatrix} \quad (24)$$

where $\nu = \int e d\tau$, K_p is a negative diagonal matrix, I_2 is a unity matrix of order 2, $0_{2 \times 2}$ is a 2 by 2 zero matrix. The controller gain matrix K_i is chosen to make the plant faster and with zero steady-state while keeping the eigenvalues of the modified plant:

$$K_i = -A_s K_p. \quad (25)$$

A. Stability issues

In this section, we study the stability properties of the closed-loop system using the control input proposed in (23) and (25). First, the considered single track model includes neither cornering force nor actuator dynamics. The closed-loop evolves as:

$$\dot{e} = (A_s + K_p)e + K_i \int e d\tau. \quad (26)$$

If (27) is differentiated once, the resulting equation

$$\ddot{e} - (A_s + K_p)\dot{e} + A_s K_p e = 0 \quad (27)$$

has the eigenvalues A_s and K_p if K_p is a diagonal matrix with negative elements.

Hence, the reduced order system is stable provided that K_p is chosen as a stable matrix.

With the controller parameters chosen, we have also verified numerically that the complex model of (12) and (13) is also stable.

B. Robustness to Parameter variations

Consider the plant described in (14) where the parameters in A_1 and B_1 are uncertain but bounded to $\pm 15\%$. As we assume that the parameters are unknown but they remain fixed with time, it is enough for the eigenvalues of the closed-loop system to be on the left-hand side of the complex plane to prove stability. Recalling that the control input is:

$$\delta^i = B_{1nom}^{-1}(\dot{x}_{ref} - A_{1nom}x + (A_{snom} + K_p)e - A_{snom}K_p \int ed\tau),$$

where A_{1nom} , A_{snom} and B_{1nom} are the A_1 , A_s and B_1 matrices, respectively, evaluated with the nominal parameters. The resulting closed-loop system is:

$$\begin{aligned} \dot{e} - (A_1 + B_1 B_{1nom}^{-1}(-A_{1nom} + A_{snom} + K_p))e \\ + B_1 B_{1nom}^{-1} A_{snom} K_p \int ed\tau = (B_1 B_{1nom}^{-1} - I)\dot{x}_{ref} \\ + (A - B_1 B_{1nom}^{-1} A_{1nom})x_{ref}. \end{aligned} \quad (28)$$

The resulting closed-loop system was evaluated for a uniform and equally spaced grid corresponding to 8^5 combinations of the 5 uncertain parameters m , I_{zz} , C_f , C_r and l_f . The closed loop eigenvalues were computed numerically for the parameter range of interest, and were checked to be in the left half of the complex plane. The same set of experiments were conducted to verify that the closed loop of the full system is also stable despite the same amount of parameter uncertainty.

Turning now to the full model in (12) and (13), we tried the same parameter variations where the tyre stiffness (C_T) at the front is calculated as:

$$C_T = \frac{C_f C_l}{2(C_l - C_f n_s)} \quad (29)$$

Finally, we have tested that the eigenvalues of the closed-loop system for the full model remain in the left-half plane with parameter uncertainty.

IV. STABILITY AND SPEED VARIATION

Previously, we assumed the vehicle speed to be constant for developing the vehicle model in (1) and (2). We will now write the equations of motion of the vehicle without the assumption of constant speed in order to analyze the stability of the controlled plant to speed variations produced by normal driving conditions involving acceleration and braking actions.

Consider the one-track model depicted in Figure 1. Notice that it includes the longitudinal tyre forces resulting from normal acceleration and braking.

For small steering angles and neglecting, the equations of motion can be linearized:

$$\dot{v}_x = v_y \dot{\psi} + \frac{F_f + F_r - S_f \delta_f - S_r \delta_r}{m} \quad (30)$$

$$\dot{v}_y = -v_x \dot{\psi} + \frac{S_f + S_r + F_f \delta_f + F_r \delta_r}{m} \quad (31)$$

$$\ddot{\psi} = \frac{S_f l_f - S_r l_r + F_f l_f \delta_f - F_r l_r \delta_r}{I_{zz}} \quad (32)$$

where F_f and F_r are the front and rear longitudinal forces, respectively.

In the general case when v_x is not fixed and considering that the cornering stiffness and actuator dynamics are fast enough to be neglected, the equations of motion for the lateral dynamics are given by

$$\dot{x}(t) = A_1(t)x + B_2(t)\delta^i \quad (33)$$

where A_1 is the same as defined earlier but time-varying and $B_2(t) = B_1 + B_v(t)$ where $B_v(t)$ is time-varying and defined as:

$$B_v(t) = \begin{bmatrix} \frac{F_f(t)}{F_f^m(t)l_f} & \frac{F_r(t)}{F_r^m(t)l_r} \\ \frac{F_f^m(t)l_f}{I_{zz}} & -\frac{F_r^m(t)l_r}{I_{zz}} \end{bmatrix} \quad (34)$$

Now let us consider the control input previously defined in (23) and (25). The resultant closed-loop system is:

$$\begin{aligned} \dot{e}(t) - (L_p(t)(A_s(t) + K_p) - T_v(t)A_1(t))e(t) + \\ L_p(t)A_s(t)K_p \int^t e(\tau)d\tau = T_v(t)(\dot{x}_{ref}(t) - A_1(t)x_{ref}) \end{aligned} \quad (35)$$

where $L_p(t) = I + B_v(t)B_1^{-1}$ and $T_v(t) = B_v(t)B_1^{-1}$. So the closed-loop system is:

$$\dot{x}_2(t) = A_{cl}(t)x_2(t) + [0, 1]^T w_{exo}, \quad (36)$$

where $x_2 = [e, \nu]'$ and the time-varying A_{cl} matrix is:

$$A_{cl}(t) = \begin{bmatrix} L_p(t)(A_s(t) + K_p) - T_v(t)A_1(t) & \\ I_2 & \\ -L_p(t)A_s(t)K_p & \\ & 0_{2 \times 2} \end{bmatrix} \quad (37)$$

and the exogenous term

$$w_{exo} = T_v(t)(\dot{x}_{ref}(t) - A_1(t)x_{ref}) \quad (38)$$

is bounded.

In order to prove that the system states remain bounded for normal driving conditions involving acceleration and braking, a Common Quadratic Lyapunov Function (CQLF) of the form $[e, \nu]^T P [e, \nu]$ with symmetric positive definite matrix P satisfying:

$$A_{cl}^T P + P A_{cl} < 0 \quad (39)$$

was found for all $v_x \in [10, 30]$, $F_f \in [-6800, 6800]$ and $F_r \in [-6800, 0]$. The common P matrix is:

$$P = \begin{bmatrix} 0.8405 & 0.0396 & 0.0149 & -0.0014 \\ 0.0396 & 0.9095 & 0.0350 & 0.0118 \\ 0.0149 & 0.0350 & 0.0294 & 0.0056 \\ -0.0014 & 0.0118 & 0.0056 & 0.0056 \end{bmatrix}. \quad (40)$$

The existence of such a CQLF guarantees the boundedness of the signals for time variations in v_x , F_f and F_r within the specified range.

V. TESTS IN AN ADVANCED NONLINEAR SIMULATION

In this section, we test the proposed controller in an advanced nonlinear full vehicle simulation. This was provided by DaimlerChrysler and is a 5-body (chassis and 4 wheels) nonlinear vehicle simulator that includes a nonlinear passive suspension, nonlinear brake models, the sensing, observer and actuation systems found in the real test car. As the simulation set-up has to be similar to the one in the real car, the lateral controller in simulation operates with a sampling time of 10ms with 20ms time-delay and side-slip angle, as it can't be measured, is obtained with a Kalman-filter observer.

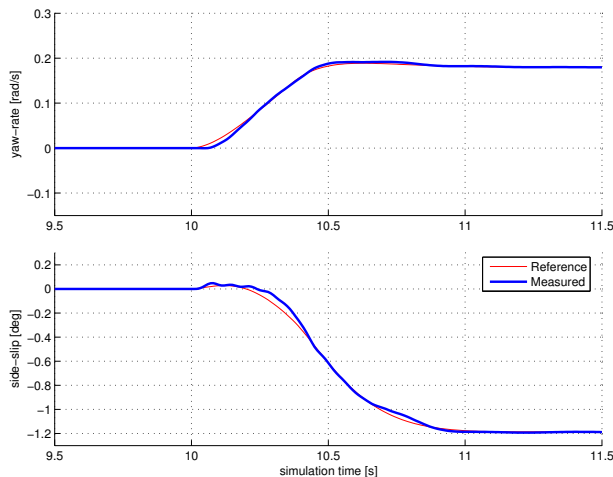


Fig. 3. Basic emulation of a large vehicle performing a J-turn maneuver

First we present the emulation response of a set of different maneuvers and vehicles. The standard maneuvers to be considered are a J-turn, slalom and a lane-change while the vehicles to be considered are mini-size, large-size and a bus. The test vehicle to be used is a medium-size vehicle equipped with 4WS and a cruise control system to keep the vehicle speed constant. In Figure 3, we perform a modified J-turn emulating a large-size vehicle. The magnitude of the maneuver was selected to reach a lateral acceleration of $4m/s^2$, i.e., the valid limits of the linear model. The mini-size vehicle states tracking is presented in Figure 4 for a slalom maneuver with a maximum lateral acceleration of $4m/s^2$ and a frequency of 0.2 Hz. Finally, a lane-change maneuver can be observed in Figure 5 for our test vehicle tracking the lateral dynamics of a bus. In all cases, the tracking is fast and with no steady-state errors.

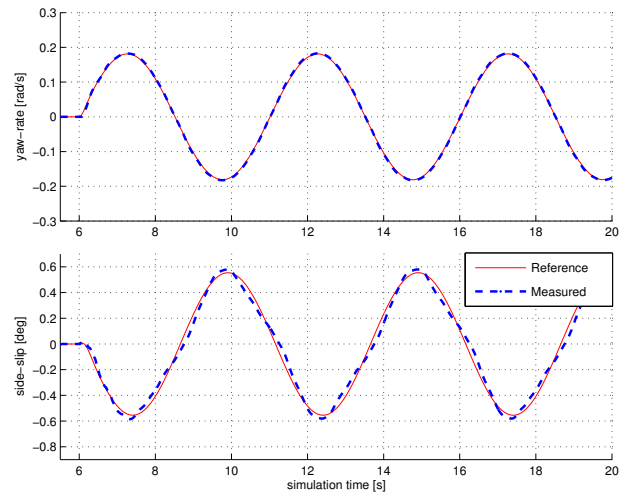


Fig. 4. Basic emulation of a mini-size vehicle performing a slalom maneuver

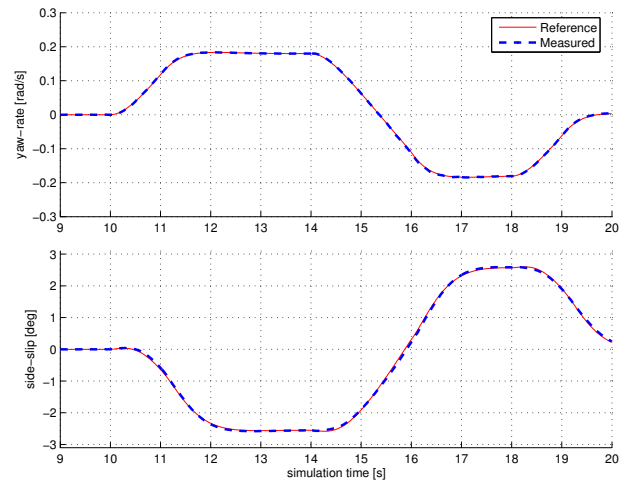


Fig. 5. Basic emulation of a bus performing a lane-change maneuver

A. Operation at varying speeds

We now consider the robustness of the closed-loop system to velocity variations. Let us recall that the speed was originally considered as a parameter. As it may be measured, the matrices used in the controller A_{1nom} and A_{snom} are implemented as a function of the measured speed v_x . The resulting controller performs well under varying velocity conditions when tested on the nonlinear simulation.

We have tested the controller for a vehicle decreasing its speed slowly while performing a J-turn with the controller tracking without affecting the tracking performance of the controller. A much harder test is presented in Figure 6. In this case, the driver keeps the speed at 80km/h as he performs a J-turn with a steering-wheel rate of 200 deg/s. He brakes just afterwards and, when the vehicle has decreased its speed around 30 km/h, the driver decides to recover his previous speed and accelerates again. The controller performs well also for this more aggressive test.

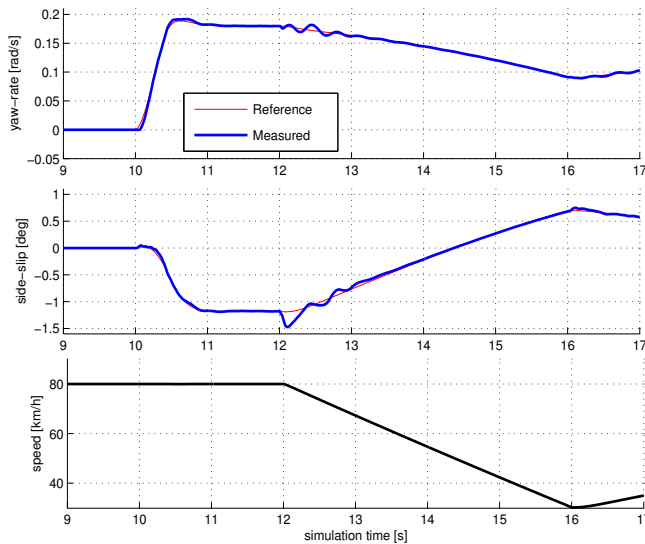


Fig. 6. Large vehicle tracking while braking in complex non linear simulation

B. Robustness to μ -split and sidewind perturbations

For the task of emulating a number of vehicles, we then test the robustness of our design with respect to common vehicle disturbances: slippery roads and wind. Roads have a specially coated surface with a high friction coefficient. The μ -split test considers the occasions when two of the wheels of the lateral vehicle go out of the road causing a difference in the friction coefficient experienced by the tyres at the left and those at the right. It would also be encountered when two of the wheels drive over a wet surface. In either of these cases, the friction coefficient difference will cause the vehicle to yaw with the driver possibly losing control of the vehicle. In Figure 7, a vehicle emulating a large vehicle and driving straight-ahead encounters a μ -splitted surface for a few meters. While one side of the car drives over a surface with friction coefficient of 1.0, the other half drives over a surface with 0.5. Afterwards, and before the driver decides to perform a J-turn maneuver, the vehicle encounters a 100 km/h sidewinder perturbation. Sidewinder perturbations can be common in highways and appear while crossing a bridge in the mountains, leaving the vehicle suddenly exposed. The vehicle in Figure 7 keeps tracking in spite of the strong sidewinder and the driver.

VI. CONCLUSIONS

In this paper, we have developed a novel control strategy for controlling a 4WS vehicle. The stability and robustness of the controller are shown to be acceptable in a complex nonlinear simulation by a car manufacturer. The application

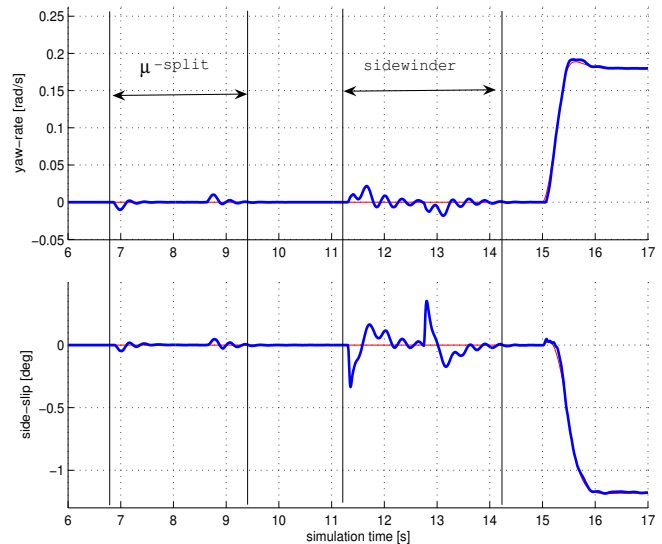


Fig. 7. Robustness to μ -split and sidewind perturbations

of one single 4WS vehicle emulating different ranges of vehicles opens new possibilities for vehicle design: from prototype vehicle testing at the limits of operation to providing an enhanced driving experience to the driver.

VII. ACKNOWLEDGEMENTS

This work was supported by EU STREP grant 004175.

REFERENCES

- [1] A. Y. Lee, A. T. Marriott, and N. T. Le, "Variable dynamic testbed vehicle: Dynamic analysis," in *Proceedings of the 1997 SAE International Congress and Exposition*, 1997. SAE Paper No. 970560.
- [2] A. Lee, "Emulating the lateral dynamics of a range of vehicles using a four-wheel-steering vehicle," in *International Congress and Exposition*, (Detroit, Michigan), 1995. SAE Paper No.950304.
- [3] L. Gianone, L. Palkovics, and J. Bokor, "Design of an active 4ws system with physical uncertainties," *Control Engineering Practice*, vol. 3, no. 8, pp. 1075–1083, 1995.
- [4] J. Ackermann, "Robust decoupling, ideal steering dynamics and yaw stabilization of 4ws cars," *Automatica*, vol. 30, pp. 1761–1768, 1994.
- [5] J. Ackermann, "Active steering for better safety, handling and comfort," in *Conference on Advances in Vehicle Control and Safety*, (Amiens, France), 1998.
- [6] D. Leith, W. Leithead, and M. Vilaplana, "Robust lateral controller for 4-wheel steer cars with actuator constraints," in *44th IEEE Conference on Decision and Control, and the European Control Conference 2005*, (Seville, Spain), pp. 6952–6957, Dec. 2005.
- [7] M. Akar, "Yaw rate and sideslip tracking for 4-wheel steering cars using sliding mode control," in *Proc. of the IEEE International Conference on Control Applications*, (Munich, Germany), Oct. 2006.
- [8] M. Barreras, C. Villegas, M. Garcia-Sanz, and J. Kalkkuhl, "Robust QFT tracking controller design for a car equipped with 4-wheel steer-by-wire," in *Proc. of the IEEE International Conference on Control Applications*, (Munich, Germany), Oct. 2006.
- [9] T. D. Gillespie, *Fundamentals of vehicle dynamics*. Society of Automotive Engineers, 1992.